SUPPLEMENTAL DATA

Table S1: Related to Figure 2. mSOD1-astrocyte induced GES.

Part A. ES-MN GES in response to mSOD1 ACM for 1 and 3 days. The table lists the entrez gene identifier, official gene symbol, moderated t-statistic and p-value estimated by the limma package (Bioconductor) and FDR for the 1d- and 3d-GES.

Part B. Differential expression of neuron-specific necroptosis genes at 3 days after mSOD1 ACM exposure. The table lists the 40 neuron-specific necroptosis genes indicating their differential expression at 3-days after mSOD1 ACM treatment (Z-score, p-value and FDR). The L-edge column indicates the fraction of the necroptosis genes that are in the leading-edge when their enrichment on the 3-GES was computed by GSEA.

Table S2: Related to Figure 3. MARINa results for all the evaluated TFs.

The table lists the Entrez Gene ID, Symbol, Normalized Enrichment Score (NES), p-value and FDR.

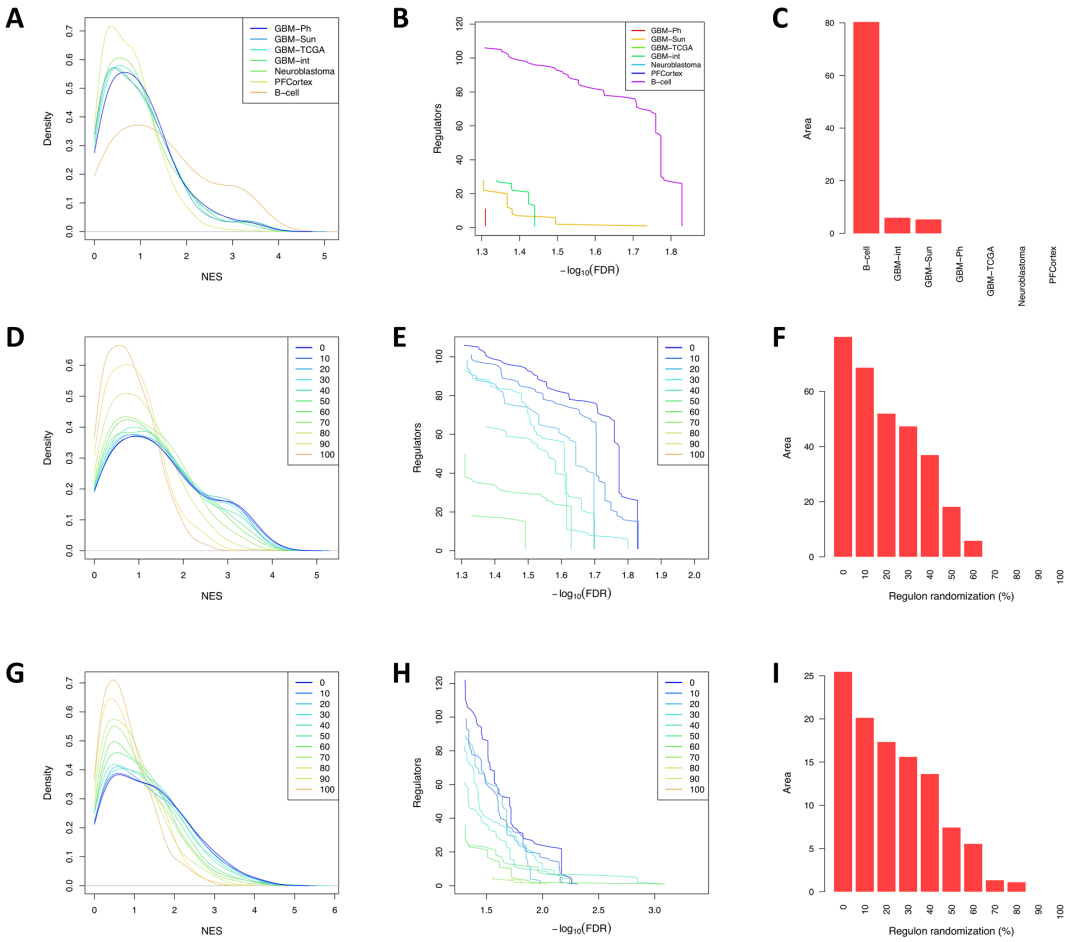

Figure S1: Related to Figure 3. Effect of tissue context specificity and partial regulon randomization on MARINa performance.
MARINa analysis was performed on a centroblasts vs. naïve B-cells GES using seven different interactomes (A-C), a partially randomized B-cell context specific interactome (D-F); or the 3-day ES-MN GES using partially randomized versions of the mouse brain interactome (G-I). Noise was progressively added to the regulons by replacing a different proportion of the target genes by genes selected at random (as indicated in the insert in panels D, E, G and H; or in the *x-axis* in panels F and I). (A, D and G) show a Gaussian kernel estimation for the probability density of the normalized enrichment score (NES) inferred by MARINa; (B, E and H) show the number of regulators inferred as differentially active (*y-axis*) at different FDR levels (*x-axis*); and (C, F and I) show the area under each of the curves shown in panels B, E and H, respectively.

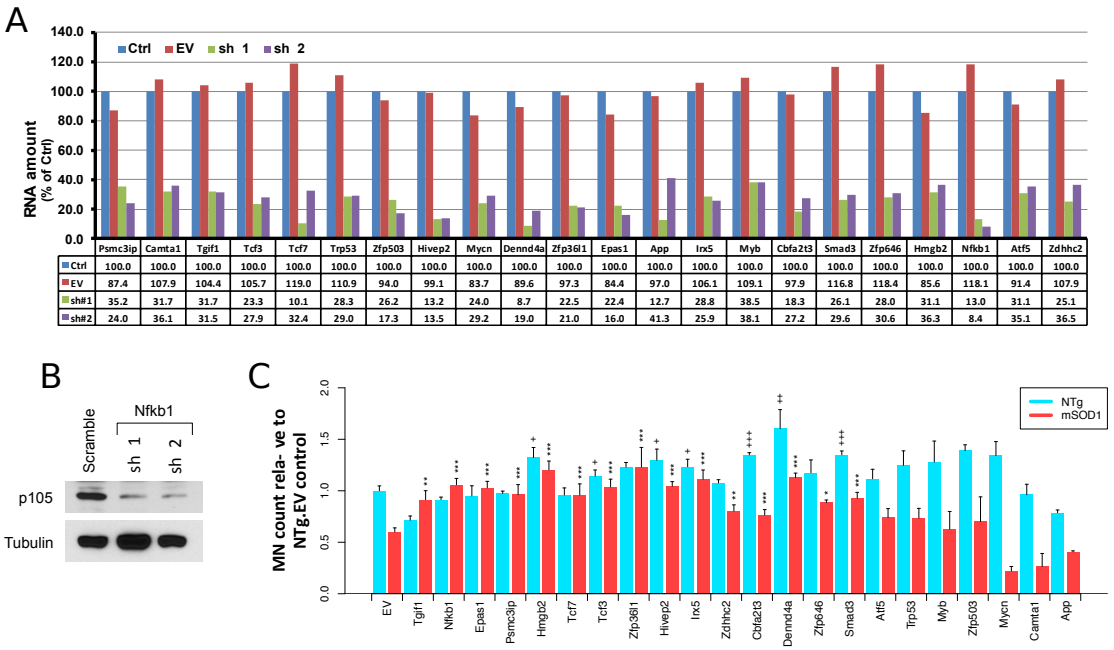

	Psmc3ip	Camta1	Tgif1	Tcf3	Tcf7	Trp53	Zfp503	Hivep2	Mycn	Dennd4a	Zfp36l1	Epas1	App	Irx5	Myb	Cbfa2t3	Smad3	Zfp646	Hmgb2	Nfkb1	Atf5	Zdhhc2
Ctrl	100.0	100.0	100.0	100.0	100.0	100.0	100.0	100.0	100.0	100.0	100.0	100.0	100.0	100.0	100.0	100.0	100.0	100.0	100.0	100.0	100.0	100.0
EV	87.4	107.9	104.4	105.7	119.0	110.9	94.0	99.1	83.7	89.6	97.3	84.4	97.0	106.1	109.1	97.9	116.8	118.4	85.6	118.1	91.4	107.9
sh#1	35.2	31.7	31.7	23.3	10.1	28.3	26.2	13.2	24.0	8.7	22.5	22.4	12.7	28.8	38.5	18.3	26.1	28.0	31.1	13.0	31.1	25.1
sh#2	24.0	36.1	31.5	27.9	32.4	29.0	17.3	13.5	29.2	19.0	21.0	16.0	41.3	25.9	38.1	27.2	29.6	30.6	36.3	8.4	35.1	36.5

Figure S2: Related to Figure 4. Validation of ALS-related Death Driver genes.
(A) Knock-down efficiency control for all the used shRNA vectors. Shown is the relative mRNA levels for each of the candidate master regulators as quantified by real-time quantitative PCR (qPCR) 48h after lentiviral mediated transduction of shRNA. The qPCR results were normalized by the housekeeping GAPDH transcript and expressed relative to non-transduced ES-MN cells (Ctrl). The bars show the mean of two independent experiments performed in triplicate for non-transduced cells (Ctrl), empty-vector transduced cells (EV) and each of the two shRNA clones directed against each gene (sh 1 and sh 2).
(B) Western blot analysis of NF-κB p105 subunit levels in ES-MNs cells 96h after lentivirus-mediated transduction of two different shRNAs against Nfkb1. α-Tubulin was used as loading control.
(C) Effect of MR knock-down on MN survival when co-cultured with NTg and mSOD1 astrocytes. Shown is the mean ± s.e.m for the ratio of the number of surviving ES-MNs following shRNA mediated knock-down of each MR relative to the EV control, when cultured on a NTg astrocyte monolayer (blue bars) or mSOD1 astrocyte monolayer (red bars). * $p < 0.05$, ** $p < 0.01$, *** $p < 0.001$ for the survival effect on mSOD1 astrocytes (i.e. ratio of the number of surviving ES-MNs following TF silencing compared to EV-transduced ones when co-cultured with mSOD1 astrocytes); $^{+}$ $p < 0.05$, $^{++}$ $p < 001$, $^{+++}$ $p < 0.001$ for the general survival effect test (i.e. ratio of surviving ES-MNs following TF silencing compared to EV-transduced ones when co-cultured with NTg astrocytes). P-values were estimated by two-way mixed effects ANOVA.

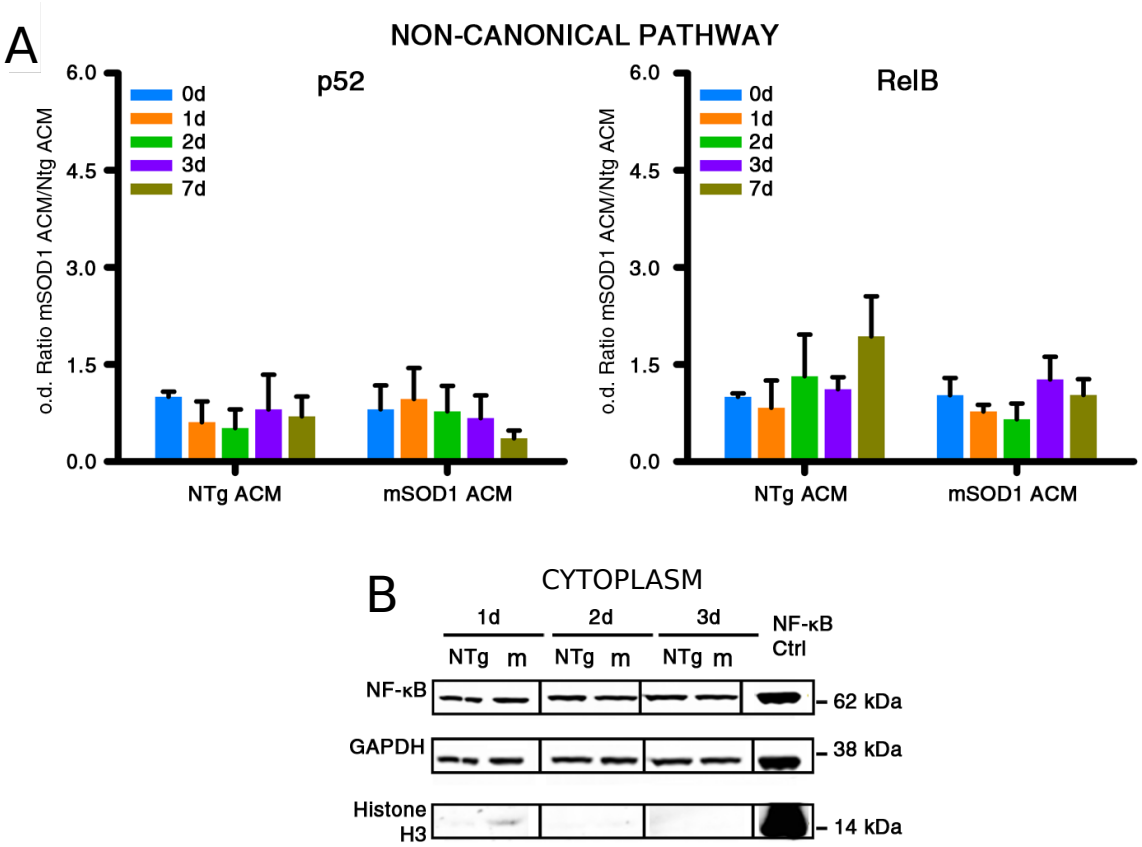

Figure S3: Related to Figure 5. NF-κB pathway is activated in ES-MNs exposed to mSOD1 ACM

(A) DNA-binding ELISA assay for the non-canonical NF-κB pathway subunits p52 and RelB in nuclear extracts from purified ES-MNs exposed to either mSOD1 ACM or NTg ACM for 0 (just before adding the ACM) to 7 days. The o.d. values are normalized to the o.d. of ES-MNs exposed to NTg ACM for 0 days.

(B) Western blot analysis for NF-κB p65 subunit content in the cytosolic fraction from purified ES-MNs exposed for 1 to 4 days to either mSOD1 or NTg ACM. GAPDH is used as housekeeping marker. NF-κB control (Ctrl) is a cell extract provided by Cell Signaling.

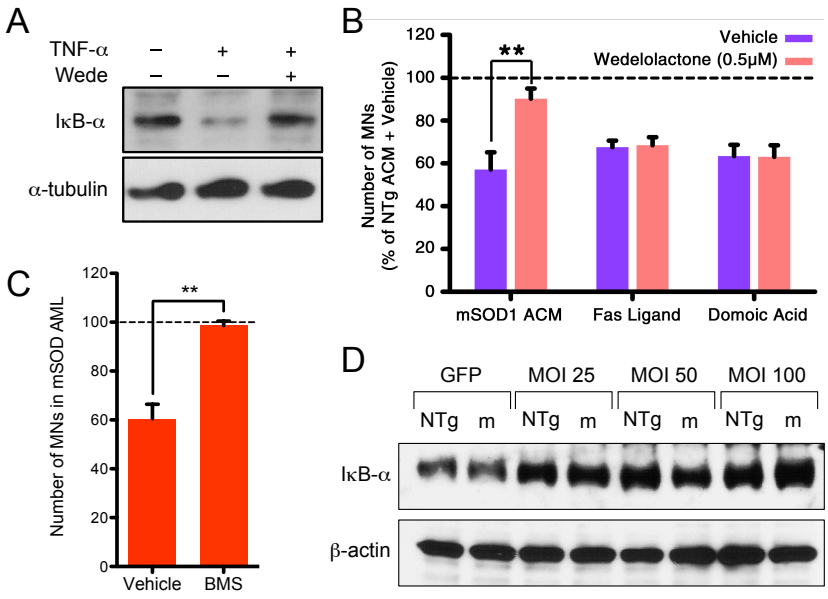

Figure S4: Related to Figure 6. Effect of wedelolactone, BMS-345541 and IκB-SR on IκB protein stability and ES-MN response to mSOD1 ACM.

(A) Western blot analysis of IκB-α protein levels in ES-MNs cells pre-incubated with Wedelolactone (Wede, 20 mM) for 1h and TNF-α (10 ng/ml) for 20 min. α-tubulin was used as loading control.

(B) Effect of 0.5 μM Wedelolactone on the loss of purified ES-MNs caused by either 7 days exposure to mSOD1 ACM or 5 days exposure to 10 ng/ml Fas ligand or 1 μM domoic acid. $^{**}p \leq 0.01$; one tail Student's t-test.

(C) Effect of 5 μM BMS-345541 on the loss of purified ES-MNs caused by 7 days exposure to mSOD1 AML. Bars represent the mean ± s.e.m. after normalization to NTg control. ** $p < 0.01$, on tail Student's t-test.

(D) Western blot analysis of IκB-α protein levels in the cytoplasmic fractions from purified ES-MNs, transduced with adenovirus expressing IκB-SR at different MOI, and exposed to either mSOD1 (m) or NTg ACM for 1 day. β-actin is the loading control.

SUPPLEMENTAL EXPERIMENTAL PROCEDURES

Minimization of the batch effect for the RNA-Seq assay, related to experimental procedures. To minimize potential batch effect, the following steps were taken in sample preparation before RNA-Seq profiling: (1) several active ACM aliquots were pooled together to generate sufficient reagent quantity for the treatment of all MNs in the study; (2) six different aliquots of ES cells, originally obtained from the same embryo, were thawed, differentiated into MNs and purified at the same time and under identical conditions; (3) all purified ES-MNs coming from the same aliquot of ES cells were plated together, exposed to ACM, and underwent processing for RNA extraction simultaneously; and (4) for each sample, RNA isolation and quality assessment was performed simultaneously.

Handling of the samples for the RNA-Seq assay, related to experimental procedures. At 1 and 3 days, cells were harvested and total mRNA was extracted from purified ES-MNs using TRI Reagent Solution (Ambion) and isolated with MagMAX-96 total RNA Isolation kit (Ambion). Note that purified ES-MNs were first plated in three adjacent wells in 12-well cell culture dishes and then their RNAs were pooled as a single sample to produce sufficient total RNA for one biological replicate. Total RNA samples were, then, quantified by Nanodrop (Thermo Scientific) and their RNA integrity was assessed using a 2100 Bioanalyzer (Agilent Technologies). High-quality total RNA samples, with RIN (RNA integrity number) above 9, were processed by the Columbia Genome Center. For each sample, a minimum of 20 million 100bp single end reads were sequenced on the Illumina HiSeq2000 platform.

Gene expression data analysis, related to experimental procedures. RNA-Seq reads were first mapped to the *Mus musculus* assembly nine reference genome, using Bowtie (Langmead et al., 2009). Reads mapping to known genes, based on Entrez gene identifiers, were then counted using the GenomicFeatures R-system package (Bioconductor (Gentleman et al., 2004)). Summarized expression data resulting from these analyses is available from the Gene Expression Omnibus database (GSE49023). Expression data was then normalized by equi-variance transformation, based on the negative binomial distribution with the DESeq R-system package (Bioconductor). This normalized data is available from figshare (http://dx.doi.org/10.6084/m9.figshare.809573). To address any residual batch effects, differential gene expression analysis was performed by fitting a two-factor, linear mixed-effects model to the normalized data, to independently estimate the variance due to treatment and to MN culture conditions (batch effect). This led to independent coefficient estimates for each gene, representing the following six culture conditions: NTg ACM (day 1; d1), wtSOD ACM (d1), mSOD1 ACM (d1), NTg ACM (day 3; d3), wtSOD1 ACM (d3) and mSOD1 ACM (d3). The relevant comparisons used to generate differential GES for d1 and d3 include:

$$mSOD1\ ACM\ d1 - \frac{NTg\ ACM\ d1 + wtSOD1\ ACM\ d1}{2}$$

and

$$mSOD1\ ACM\ d3 - \frac{NTg\ ACM\ d3 + wtSOD1\ ACM\ d3}{2}$$

respectively. In these, the NTg ACM and wtSOD1 ACM treatments were averaged to generate a representative control condition. Statistical significance was estimated by a

moderated Student's *t*-test implemented in the limma package (Dudoit et al., 2003) for the R-system (Bioconductor).

Enrichment of the 1-GES and 3-GES on a set of 40 neuron-specific necroptosis associated genes (Hitomi et al., 2008) was performed by Gene Set Enrichment Analysis as described in the original publication (Subramanian et al., 2005).

Reverse engineering of context-specific transcriptional interactomes, related to experimental procedures. Interactomes were reverse engineered by ARACNe (Margolin et al., 2006) from six different GEP data sets (see Supplemental Experimental Procedures). ARACNe was run with 100 bootstrap iterations using all probes that could be mapped to a set of 1,857 human transcription factors, i.e., genes annotated in Gene Ontology Molecular Function database (Ashburner et al., 2000) as GO:0003700 – 'transcription factor activity', or as GO:0004677 – 'DNA binding' and GO:0030528 – 'Transcription regulator activity', or as GO:0004677 and GO: 0045449 – 'Regulation of transcription') for the human datasets, or 1,507 mouse transcription factors for the mouse brain dataset. Parameters were set to 0 DPI tolerance and a MI *p*-value threshold ($p < 10^{-7}$), as recommended for bootstrap ARACNe analysis of a dataset of this size, to achieve Bonferroni corrected significance ($p = 0.05$) for getting a single false-positive in the network. Human interactome genes were mapped to their mouse orthologs by using the HomoloGene database (http://www.ncbi.nlm.nih.gov/homologene). All the interactomes used in this publication are available for download from figshare (http://dx.doi.org/10.6084/m9.figshare.809573).

MAster Regulator INference algorithm (MARINa), related to experimental procedures. The MARINa algorithm used for this publication is an improved version of

the original algorithm (Carro et al., 2010; Lefebvre et al., 2010) with the following modifications: (1) it tests for a global shift in the position of the regulons when projected on the GES instead of the Kolmorogov-Smirnov test statistics; (2) it test the enrichment of each tail, or globally, according to the regulator mode of action, either activator, repressor or mixed, respectively; (3) takes into account pleiotropic regulation of each target gene by multiple regulators when computing the enrichment. Statistical significance, including p-value and normalized enrichment score (NES), is estimated by comparison to a null model generated by permuting the samples uniformly at random 1,000 times. The MARINa algorithm is implemented in the "ssmarina" R-package available for download from figshare (http://dx.doi.org/10.6084/m9.figshare.785718).

Transcriptional interactomes assembled for this work, Related to Experimental Procedures

Interactome	Dataset	Samples	Transcription factors	Targets	Interactions
GBM-Ph	Human glioblastoma (Phillips et al., 2006)	176	416	3,222	35,198
GBM-Sun	Human glioma (Madhavan et al., 2009)	427	608	5,039	83,526
GBM-TCGA	Human glioblastoma TCGA Affymetrix dataset	516	766	6,268	209,589
GBM-Int	Human integrated glioma (gbm-hgg176 + gbm-sun + gbm-tcga)	1,119	632	5,287	157,321
Neuroblastoma	Human neuroblastoma (NCI-OCG-TARGET program http://ocg.cancer.gov/programs/target)	189	663	5,407	83,155
PFCortex	Human prefrontal cortex (http://dx.doi.org/10.7303/syn4505.1)	153	773	6,318	183,837
$Brain^{Net}$	Mouse brain (GSE10415)	437	1,345	15,700	368,471

Availability: http://dx.doi.org/10.6084/m9.figshare.809573

shRNA pLKO.1 clones used in this work, Related to Experimental Procedures

Gene Symbol	TRC ID from Sigma Mission
Camta1	TRCN0000231368
Camta1	TRCN0000231367
Dennd4a	TRCN0000341323
Dennd4a	TRCN0000341381
Zfp36l1	TRCN0000123469
Zfp36l1	TRCN0000238293
Hmgb2	TRCN0000304268
Hmgb2	TRCN0000301407
Zfp239	TRCN0000082328
Zfp239	TRCN0000082330
Mycn	TRCN0000042523
Mycn	TRCN0000042524
Psmc3ip	TRCN0000120273
Psmc3ip	TRCN0000120275
Tcf7	TRCN0000262741
Tcf7	TRCN0000262740
Tgif1	TRCN0000055048
Tgif1	TRCN0000055050
Cbfa2t3	TRCN0000096429
Cbfa2t3	TRCN0000096431
Epas1	TRCN0000082303
Epas1	TRCN0000082304
Hivep2	TRCN0000095774
Hivep2	TRCN0000095777
Myb	TRCN0000042498
Myb	TRCN0000042500
Tcf3	TRCN0000233414
Tcf3	TRCN0000233413
Trp53	TRCN0000304241
Trp53	TRCN0000012359
Smad3	TRCN0000089023
Smad3	TRCN0000089027
Irx5	TRCN0000070420
Irx5	TRCN0000348102
Aatf	TRCN0000086033
Aatf	TRCN0000086034
Atf5	TRCN0000075553
Atf5	TRCN0000075555
Zfp503	TRCN0000071943
Zfp503	TRCN0000071945
Zfp646	TRCN0000084683
Zfp646	TRCN0000084684
Zdhhc2	TRCN0000124889
Zdhhc2	TRCN0000124890
App	TRCN0000054873
App	TRCN0000054877
Nfkb1	TRCN0000009510
Nfkb1	TRCN0000009512

SUPPLEMENTAL REFERENCES

Ashburner, M., Ball, C.A., Blake, J.A., Botstein, D., Butler, H., Cherry, J.M., Davis, A.P., Dolinski, K., Dwight, S.S., Eppig, J.T.*, et al.* (2000). Gene ontology: tool for the unification of biology. The Gene Ontology Consortium. Nat Genet *25*, 25-29.

Carro, M.S., Lim, W.K., Alvarez, M.J., Bollo, R.J., Zhao, X., Snyder, E.Y., Sulman, E.P., Anne, S.L., Doetsch, F., Colman, H.*, et al.* (2010). The transcriptional network for mesenchymal transformation of brain tumours. Nature *463*, 318-325.

Dudoit, S., Gentleman, R.C., and Quackenbush, J. (2003). Open source software for the analysis of microarray data. BioTechniques *Suppl*, 45-51.

Gentleman, R.C., Carey, V.J., Bates, D.M., Bolstad, B., Dettling, M., Dudoit, S., Ellis, B., Gautier, L., Ge, Y., Gentry, J.*, et al.* (2004). Bioconductor: open software development for computational biology and bioinformatics. Genome Biol *5*, R80.

Hitomi, J., Christofferson, D.E., Ng, A., Yao, J., Degterev, A., Xavier, R.J., and Yuan, J. (2008). Identification of a molecular signaling network that regulates a cellular necrotic cell death pathway. Cell *135*, 1311-1323.

Langmead, B., Trapnell, C., Pop, M., and Salzberg, S.L. (2009). Ultrafast and memory-efficient alignment of short DNA sequences to the human genome. Genome Biol *10*, R25.

Lefebvre, C., Rajbhandari, P., Alvarez, M.J., Bandaru, P., Lim, W.K., Sato, M., Wang, K., Sumazin, P., Kustagi, M., Bisikirska, B.C.*, et al.* (2010). A human B-cell interactome identifies MYB and FOXM1 as master regulators of proliferation in germinal centers. Mol Syst Biol *6*, 377.

Madhavan, S., Zenklusen, J.C., Kotliarov, Y., Sahni, H., Fine, H.A., and Buetow, K. (2009). Rembrandt: helping personalized medicine become a reality through integrative translational research. Molecular cancer research : MCR *7*, 157-167.

Margolin, A.A., Nemenman, I., Basso, K., Wiggins, C., Stolovitzky, G., Dalla Favera, R., and Califano, A. (2006). ARACNE: an algorithm for the reconstruction of gene regulatory networks in a mammalian cellular context. BMC bioinformatics *7 Suppl 1*, S7.

Phillips, H.S., Kharbanda, S., Chen, R., Forrest, W.F., Soriano, R.H., Wu, T.D., Misra, A., Nigro, J.M., Colman, H., Soroceanu, L.*, et al.* (2006). Molecular subclasses of high-grade glioma predict prognosis, delineate a pattern of disease progression, and resemble stages in neurogenesis. Cancer Cell *9*, 157-173.

Subramanian, A., Tamayo, P., Mootha, V.K., Mukherjee, S., Ebert, B.L., Gillette, M.A., Paulovich, A., Pomeroy, S.L., Golub, T.R., Lander, E.S.*, et al.* (2005). Gene set enrichment analysis: a knowledge-based approach for interpreting genome-wide expression profiles. Proc Natl Acad Sci USA *102*, 15545-15550.